# Hybrid energy storage system for dynamic power management in grid-connected microgrid

**Yaya Kamagaté[1], Heli Amit Shah[2]**
[1]Department of Electrical Engineering, Parul University, Vadodara, India
[2]Department of Robotics and Automation Engineering, Parul University, Vadodara, India

| Article Info | ABSTRACT |
|---|---|
| | This paper presents an adaptive rule-based approach for dynamic power management in grid-connected microgrids. Solar photovoltaics (PV) and a battery-ultracapacitor hybrid energy storage system form the DC subsystem. Initially, the reference power is processed through a low-pass filter, diverting high-frequency power variations to the ultracapacitor, thereby safeguarding the battery. Then, a power allocation factor proportional to the battery state of charge manages the average power distribution between the battery and the grid. Finally, a microgrid power management system (MPMS) establishes rules to regulate power sharing among sources and loads. In the proposed method, the battery handles long-term energy requirements, the ultracapacitor meets short-term power demands, and the grid is adjusted to align with the system's requirements. The main benefits involve effective power distribution among sources and loads, DC bus voltage stabilization, smooth transitions between different operating modes, and enhanced grid power quality. Additionally, safety protocols prevent overcharging/deep discharging, thus reducing the risk of premature degradation and resulting in longer lifespan of storage devices. MATLAB/Simulink is used to implement and validate the method. |

*Corresponding Author:*

Yaya Kamagaté
Department of Electrical Engineering, Parul University
Vadodara, India
Email: 200300418001@paruluniversity.ac.in

## NOMENCLATURE

| | | | |
|---|---|---|---|
| HESS | : Hybrid energy storage system | $i_{rgr}$ | : Grid reference current |
| MPMS | : Microgrid power management system | $I_{abc}$ | : Inverter three-phase currents |
| DP | : Deficit power | $i_d, i_q$ | : dq current coordinates |
| SP | : Surplus power | $i_{rd}, i_{rq}$ | : dq reference current coordinates |
| $\alpha$ | : Power allocation factor | $V_{dc}$ | : DC bus voltage |
| $\tau$ | : LPF time constant | $V_{rdc}$ | : Reference DC bus voltage |
| $\omega t$ | : Reference phase angle | $V_{pv}$ | : PV voltage |
| $SoC_{bt}$ | : Battery state of charge | $V_{bt}$ | : Battery voltage |
| $SoC_{uc}$ | : Ultracapacitor state of charge | $V_{uc}$ | : Ultracapacitor voltage |
| $I_{rtot}$ | : Total reference current | $V_{gr}$ | : Grid phase voltage |
| $I_o$ | : DC subsystem output current | $V_{rd}, V_{rq}$ | : dq reference voltages |
| $i_{pv}$ | : PV current | $V_{ra}, V_{rb}, V_{rc}$ | : Three-phase reference voltages |
| $i_{bt}$ | : Battery current | $P_{pv}$ | : PV power |
| $i_{uc}$ | : Ultracapacitor current | $P_{acl}$ | : AC load power |

| $i_{rbt}$ | : Battery reference current | $P_{dcl}$ | : DC load power |
|---|---|---|---|
| $i_{ruc}$ | : Ultracapacitor reference current | $P_{tl}$ | : Total load power |
| $P_{avg}$ | : Average power | $P_{ruc}$ | : Generated ultracapacitor reference power |
| $P_{tran}$ | : Transient power | $P_{rgr}$ | : Generated grid reference power |
| $P_{bt}$ | : Battery power | $P_{dif}$ | : Power difference between PV power and total load power |
| $P_{ucr}$ | : Resultant ultracapacitor power | $P_{btn}$ | : Battery-rated charging power |
| $P_{btr}$ | : Resultant battery power | $P_{ucn}$ | : Ultracapacitor-rated charging power |
| $P_{grr}$ | : Resultant grid power | $P_{gr}$ | : Grid power |
| $P_{bt\_er}$ | : Battery power error | $P_{uc}$ | : Ultracapacitor power |
| $P_{rbt}$ | : Generated battery reference power | $P_{rtot}$ | : Total reference power |

# 1. INTRODUCTION

According to the International Energy Agency (IEA), power generation is the leading contributor to global carbon dioxide ($CO_2$) emissions. However, it is also spearheading the shift towards net zero emissions, driven by the rapid growth of renewable energy sources, with the fundamental challenge being to provide consumers with reliable and affordable electricity while simultaneously reducing worldwide $CO_2$ emissions [1]. Renewable energy sources present environmentally friendly alternatives to fossil fuels, helping to reduce carbon emissions, enhance energy security, support economic growth, mitigate climate change, and improve electricity accessibility in remote areas. Therefore, developing renewable energy sources is essential for creating sustainable, economical, reliable, and efficient energy systems. Despite these benefits, renewable energy sources' intermittent and unpredictable nature poses challenges related to reliability, stability, and power quality [2]. Energy storage elements offer a viable solution to these challenges by ensuring a stable and continuous electricity supply [3], [4]. Various energy storage systems have been explored in the literature to address these concerns [5]. However, no single energy storage system can fully meet all operational requirements due to limitations in power density, energy density, cost, lifespan, dynamic response, and other factors [6].

A hybrid energy storage system (HESS), which combines two or more storage systems, emerges as a viable solution to address these limitations and the associated trade-offs [7], [8]. Among the various storage combinations explored in the literature, the battery-ultracapacitor pair has demonstrated significant results, with the battery providing average energy needs and the ultracapacitor handling fluctuating power demands [9], [10]. Integrating diverse energy sources and loads further increases microgrid system complexity and presents substantial challenges for power management and operational security [11]. This involves ensuring continuous and efficient power distribution while safeguarding all energy sources, particularly storage devices, which need protection to prevent premature degradation and extend their lifespan [12]. Additionally, connecting the DC subsystem to the utility grid introduces challenges related to grid synchronization and reactive power control. Addressing these challenges is crucial for maintaining system reliability, efficiency, and stability and enhancing overall microgrid performance. Numerous methods have been proposed in the literature to tackle these issues, offering potential solutions for improved microgrid operation.

A coordinated control-based energy management method is proposed for a microgrid configuration featuring a photovoltaic system, battery storage, and supercapacitor (SC) storage, operating in both grid-connected and standalone modes [13]. The method employs a dual-cascaded proportional-integral (PI) controller scheme. This maintains a constant DC link voltage, ensures grid stability across various operating modes, and achieves a grid unity power factor. However, the study does not control storage devices' charge states, which could result in early deterioration and insufficient energy for future demands.

An efficient energy management algorithm for a mobile hospital is proposed in [14]. The approach aims to regulate power converters and maintain uninterrupted power transfer among the system elements. The method maintains a constant DC bus voltage and ensures that storage devices' states of charge (SoCs) operate within safe limits. However, disconnecting specific loads in light of the battery's SoC can result in hazardous situations for patients and staff.

A novel power management strategy is introduced in [15] to overcome generation-demand imbalance and regulate DC bus voltage. The approach implements a power distribution strategy between the battery and the supercapacitor, which improves the DC bus voltage regulation, minimizes battery stress, and extends the battery lifespan. Compared to the conventional method, this method demonstrates superior performance. However, the authors did not evaluate the system's performance when the states of charge of storage devices reached their safe operating limits.

A power management strategy for military microgrids is proposed in [16]. The approach enhances battery longevity, regulates the supercapacitor (SC) current, and prevents SC overcharging, ensuring uninterrupted system operation even when the SC hits its lower threshold. The method also connects HESS

management with economic outcomes by conducting a sensitivity analysis to evaluate yearly financial returns. However, the SC's transition between charging and discharging modes is strongly influenced by the gain parameter in current regulation.

An SoC-based linear time-varying filter is introduced in [17] to smooth a wind turbine/HESS output power. The approach improves the power smoothing ability of the HESS by modifying the filter's time constants based on fluctuations in the state of charge of the energy storage devices. However, the approach is primarily configured for power smoothing and is unsuitable for dynamic power balancing applications.

A strategy for the design and control of a hybrid renewable system featuring a battery and supercapacitor is proposed in [18]. The approach efficiently balances power, enhances dynamic response, stabilizes the DC bus voltage, and maintains consistent load voltage and frequency under load disturbances and varying weather conditions. However, the method does not manage SoCs, which could result in early deterioration of storage elements and energy shortages for future demands.

An efficient energy management strategy is proposed, which regulates the power exchange between the battery and the ultracapacitor [19]. This control technique ensures a balanced power flow and minimizes fluctuations within the system. However, it does not consider the ultracapacitor's state of charge, which may lead to insufficient power for future demands.

Advanced techniques have been proposed to address the shortcomings of traditional methods. However, these methods have their specific challenges. For instance, the effectiveness of artificial neural networks [20], [21] relies heavily on the quality of the training data, model predictive control [22]-[24] involves complex mathematical approaches and considerable computational resources and deploying fuzzy logic control [25]-[27] in real-time presents substantial difficulties.

This research tackles these challenges by introducing a versatile power management strategy that integrates filtration, a power allocation factor, and a microgrid power management system (MPMS) to dynamically and efficiently manage and distribute microgrid power. Here are the features of the strategy: i) Efficient power distribution among sources and loads across various operating modes and smooth transitions between modes; ii) DC bus voltage stabilization regardless of operating conditions; iii) Safe operation of storage devices; and iv) Enhanced grid power quality. The paper proceeds as follows: Section 2 presents the microgrid architecture. Section 3 elaborates on the power management strategy. Section 4 showcases and examines the results. The concluding observations are presented in the final section.

## 2.    MICROGRID ARCHITECTURE

Figure 1 (see in Appendix) illustrates the microgrid system simulation setup in MATLAB/Simulink. It comprises a PV generator, battery, and ultracapacitor. The PV source is connected to the DC link through a boost converter. Bidirectional converters connect the battery and UC to the DC link, enabling two-way power flow. Additionally, a grid inverter links the utility grid to the DC link.

The incremental conductance maximum power point tracking algorithm [28] maximizes power extraction from the PV generator. The algorithm is relatively simple, relying only on the PV voltage and current for maximum power extraction. In the setup, the battery meets average energy requirements, the UC handles fluctuating power needs, while the grid's contribution is dynamically adjusted to match the overall system needs. Tata power solar systems TP300LBZ PV module, lithium-ion battery, ultracapacitor, and other components are all configured using the MATLAB/Simulink library.

## 3.    POWER MANAGEMENT STRATEGY

The overall control technique is illustrated in Figure 2. A triple proportional-integral (PI) control loop strategy is employed. It comprises one voltage control loop and two current control loops. The low-pass filter (LPF) splits the reference power into average (low-frequency) and transient (high-frequency) components. The average power is distributed between the battery and the grid using the power allocation factor ($\alpha$). The MPMS establishes rules and provides signals for generating switching pulses for buck-boost converters and the grid inverter.

### 3.1.  Control of DC link voltage and generation of pulse signals

Power balance should be maintained in the microgrid to ensure a constant DC link voltage. This principle is expressed in (1).

$$P_{dif}(t) = P_{pv}(t) - \left(P_{acl}(t) + P_{dcl}(t)\right) = P_{bt}(t) + P_{uc}(t) + P_{gr}(t) = P_{avg}(t) + P_{tran}(t), \qquad (1)$$

$P_{pv}(t)$, $P_{gr}(t)$, $P_{bt}(t)$, $P_{uc}(t)$, $P_{acl}(t)$, $P_{avg}(t)$, $P_{dcl}(t)$, $P_{tran}(t)$, $P_{dif}(t)$ are instantaneous PV power, grid power, battery power, ultracapacitor power, AC load power, average power demand, DC load power, transient power demand, and power difference, respectively; AC and DC loads form the total load ($P_{tl} = P_{acl} + P_{dcl}$).
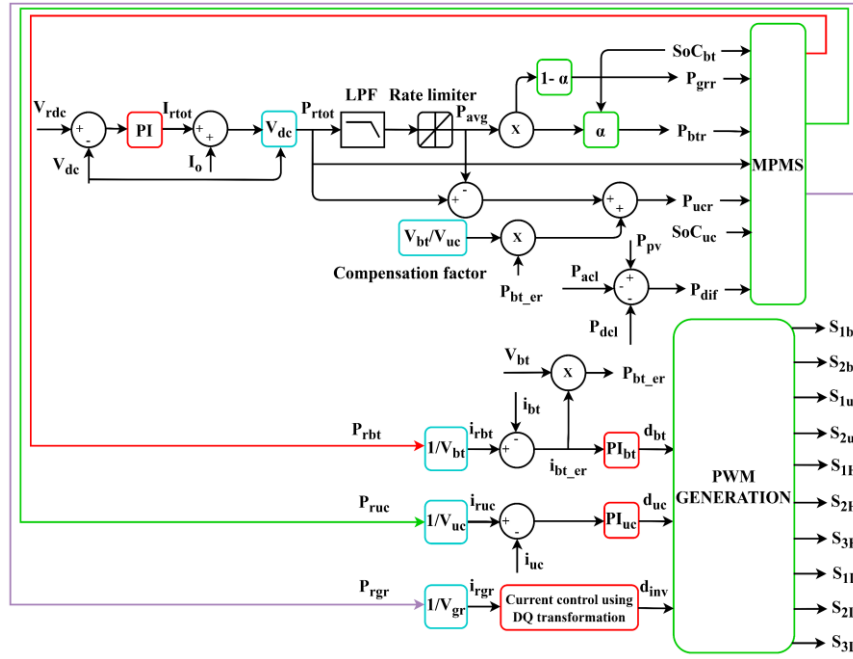
Figure 2. Proposed control strategy

From the voltage control loop, the total reference current ($I_{rtot}$) is as in (2).

$$I_{rtot}(s) = \left(K_P + \frac{K_I}{s}\right)(V_{rdc} - V_{dc}),\tag{2}$$

$K_P$ and $K_I$ are the PI controller proportional and integral parameters, whereas $V_{rdc}$ and $V_{dc}$ represent the reference and actual DC bus voltages. The total reference power ($P_{rtot}$) is given in (3) [29].

$$P_{rtot} = (I_{rtot} + I_o) * V_{dc},\tag{3}$$

$I_o$ is the output current. The total reference power ($P_{rtot}$) is separated into average power and transient power components using the LPF. The transient power is assigned to the UC, while the battery and grid share the average power. The (4)-(7) demonstrate this process.

$$P_{avg}(s) = \frac{1}{1+s.\tau} P_{rtot}(s),\tag{4}$$

$$P_{btr}(s) = \alpha. P_{avg}(s),\tag{5}$$

$$P_{grr}(s) = (1 - \alpha). P_{avg}(s),\tag{6}$$

$$P_{ucr}(s) = \left(1 - \frac{1}{1+s\tau}\right). P_{rtot}(s) + \frac{V_{bt}}{V_{uc}} * P_{bt\_er},\tag{7}$$

$\tau$ is the LPF time constant. $P_{btr}$, $P_{ucr}$, and $P_{grr}$ represent the resultant powers of the battery, UC, and grid, respectively. They serve as inputs for the MPMS. $V_{bt}$ is the battery voltage, $V_{uc}$ is the UC voltage, and $P_{bt\_er}$ is the battery power error. An additional term in the resultant UC power calculation is introduced to address the battery's slow response. The proposed power allocation factor ($\alpha$), shown in Figure 3, is determined as in (8).

$$\alpha = subplus(0.0125 * (SoC_{bt}) - 0.25),\tag{8}$$

$SoC_{bt}$ is the battery state of charge, and $0 \leq \alpha \leq 1$. MPMS uses the required parameters to generate battery ($P_{rbt}$), ultracapacitor ($P_{ruc}$), and grid ($P_{rgr}$) reference powers, which are further converted to their equivalent reference currents ($i_{rbt}$, $i_{ruc}$, and $i_{rgr}$). Pulse signals for bidirectional converters are generated by comparing the actual ($i_{bt}$ and $i_{uc}$) and obtained reference currents ($i_{rbt}$ and $i_{ruc}$) of storage devices. The following section will discuss pulse generation for the grid inverter.
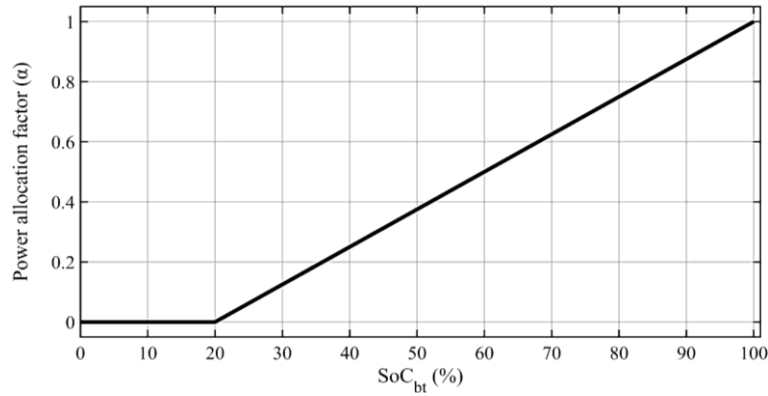
Figure 3. Proposed power allocation factor

## 3.2. Grid inverter control

The strategy utilizes a vector control approach [30] to manage the power interchange between the DC and AC subsystems, as illustrated in Figure 4. The inverter currents ($I_{abc}$) regulate both active and reactive power exchanges. dq current coordinates are obtained from the decomposition of the three-phase current coordinates ($I_{abc}$) using Park transformation. These currents ($i_d$ and $i_q$) are then compared with their references ($i_{rd}$ and $i_{rq}$), and the resulting error signals are processed through PI controllers for generating dq reference voltages ($V_{rd}$ and $V_{rq}$). Inverse Park transformation is then applied to obtain the reference three-phase voltages ($V_{ra}$, $V_{rb}$, and $V_{rc}$) for generating the inverter's switching pulses. The phase-locked loop (PLL) technique is used to obtain the appropriate reference phase angle ($\omega t$) for Park and inverse Park transformations. The strategy aims to achieve a grid unity power factor. Hence, only active power is sent to the grid by setting the q-axis (controls reactive power) reference current to zero ($i_{rq} = 0$). The reference current for the d-axis (controls active power) is set equal to the incoming current ($i_{rd} = i_{rgr}$), thereby regulating the DC bus voltage.
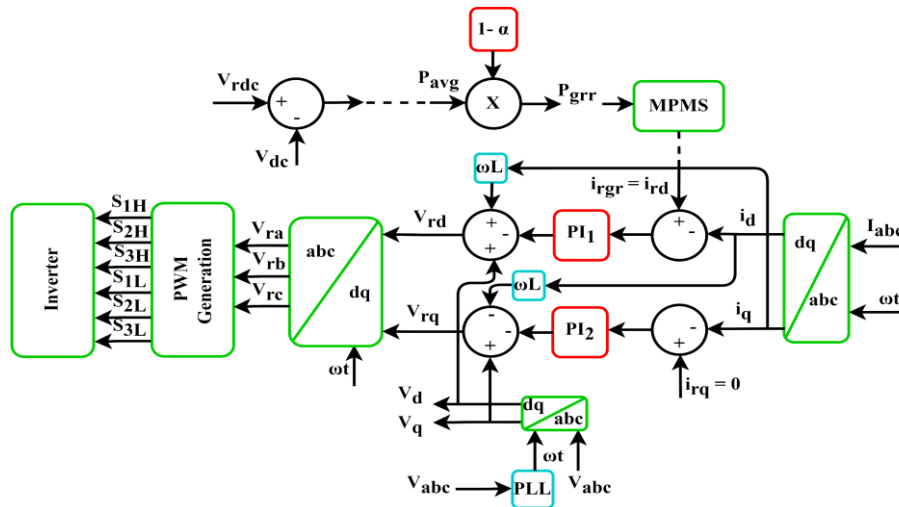


Figure 4. Inverter control block diagram

## 3.3. Microgrid power management system (MPMS)

The operation of the microgrid power management system is illustrated in the flowchart in Figure 5. MPMS is crucial for maintaining optimal power distribution between all components and ensuring their safety. It gathers data from components and makes appropriate decisions. The two modes envisaged are surplus power and deficit power. The difference between generation and consumption determines the operating mode, and storage devices' SoCs define the case. In surplus power, PV power exceeds total load power (i.e., $P_{dif} > 0$), while in deficit power, PV power is insufficient to meet the total load power (i.e., $P_{dif} < 0$). The different operating modes are explained below. $P_{btn}$ (battery) and $P_{ucn}$ (UC) represent the storage devices' rated charging powers, and $SoC_{uc}$ is the UC state of charge.

a. Surplus power: $P_{pv} > P_{tl}$
   - Case 1: $SoC_{bt} < 90\%$ and $SoC_{uc} < 95\%$, $P_{rbt} = -P_{btn}$; $P_{ruc} = -P_{ucn} + P_{ucr}$; $P_{rgr} = P_{rtot}$. Extra PV power charges storage devices, and any leftover power is fed into the grid. The grid provides extra power to cover average demands if needed, while the UC handles demands for transient power.
   - Case 2: $SoC_{bt} > 90\%$ and $SoC_{uc} < 95\%$, $P_{rbt} = 0$; $P_{ruc} = -P_{ucn} + P_{ucr}$; $P_{rgr} = P_{rtot}$. Extra PV power charges the UC, and any leftover power is fed into the grid. The grid satisfies demands for average power, and the UC addresses demands for transient power while the battery remains inactive.
   - Case 3: $SoC_{bt} < 90\%$ and $SoC_{uc} > 95\%$, $P_{rbt} = -P_{btn}$; $P_{ruc} = 0$; $P_{rgr} = P_{rtot} + P_{ucr}$. Extra PV power charges the battery, and any leftover power is fed into the grid. The grid handles demands for fluctuating power and, if needed, supplies power to meet average demands while the UC remains inactive.
   - Case 4: $SoC_{bt} > 90\%$ and $SoC_{uc} > 95\%$, $P_{rbt} = 0$; $P_{ruc} = 0$; $P_{rgr} = P_{rtot} + P_{ucr}$. Extra PV power is fed into the grid. The grid addresses transient power demands while the battery and UC remain inactive.

b. Deficit power: $P_{pv} < P_{tl}$
   - Case 1: $SoC_{bt} > 20\%$ and $SoC_{uc} > 50\%$, $P_{rbt} = P_{btr}$; $P_{ruc} = P_{ucr}$; $P_{rgr} = P_{grr}$. The battery and grid address average power demands, and UC meets transient demands.
   - Case 2: $SoC_{bt} < 20\%$ and $SoC_{uc} > 50\%$, $P_{rbt} = 0$; $P_{ruc} = P_{ucr}$; $P_{rgr} = P_{avg}$. The grid addresses average power demands, and the UC meets transient power demands while the battery remains inactive.
   - Case 3: $SoC_{bt} > 20\%$ and $SoC_{uc} < 50\%$, $P_{rbt} = P_{btr}$; $P_{ruc} = 0$; $P_{rgr} = P_{grr} + P_{ucr}$. The battery and grid address average power demands. The grid meets transient power demands while the UC is inactive.
   - Case 4: $SoC_{bt} < 20\%$ and $SoC_{uc} < 50\%$, $P_{rbt} = 0$; $P_{ruc} = 0$; $P_{rgr} = P_{avg} + P_{ucr}$. The grid meets average and transient power demands while the battery and UC are inactive.
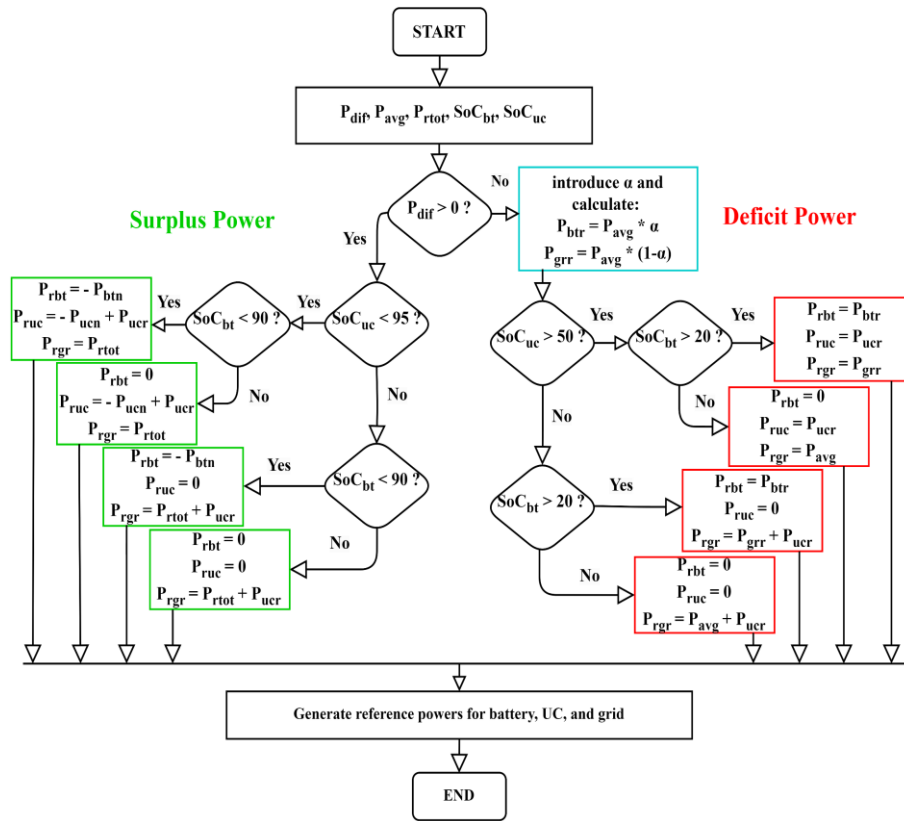


Figure 5. Flowchart of the proposed MPMS

## 4. RESULTS AND DISCUSSION

Table 1 outlines design specifications. The system is evaluated by changing solar irradiance while keeping the temperature constant at 25 °C. Figure 6 depicts the solar irradiance profile. The system is assessed for both surplus power (SP) and deficit power (DP) modes with transitions between these states.

Table 1. Design specifications

| Elements | Parameters | Values | Elements | Parameters | Values |
|---|---|---|---|---|---|
| PV module | Parallel string | 1 | Controllers | Voltage | $K_p = 0.005$; $K_i = 1.5$ |
| | Series-connected modules per strings | 11 | | Battery | $K_p = 0.1$; $K_i = 50$ |
| | | | | UC | $K_p = 0.1$; $K_i = 100$ |
| Li-ion battery | Capacity | 7 Ah | UC | Capacitance | 58 F |
| | Voltage | 240 V | | Voltage | 320 V |
| LC filter | Inductor | $L_f = 150e\text{-}3$ H | Grid | Phase voltage | 230 V |
| | Capacitor | $C_f = 1.9e\text{-}7$ F | | Frequency | 50 Hz |
| DC bus | Voltage | 700 V | Loads | DC load | 1 kW |
| | Capacitor | $C_{dc} = 10.3e\text{-}6$ F | | AC load | 0.5 kW |
| Converters | PV module | $L_{pv} = 21.4e\text{-}3$ H | | | |
| | | $C_{pv} = 2.9e\text{-}6$ F | | | |
| | Battery | $L_{bt} = 15.4e\text{-}3$ H | | | |
| | UC | $L_{uc} = 12.6e\text{-}3$ H | | | |
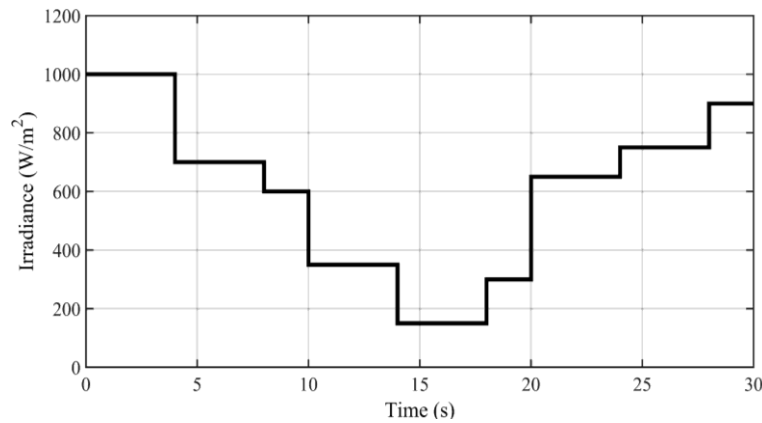


Figure 6. Solar irradiance profile

## 4.1. Simulation results

Figures 7-11 showcase the results. From 0 s to $t_4$ and from $t_8$ to 30 s, the system operates in SP mode, while between $t_4$ and $t_8$, it operates in DP mode. From 0 s to $t_1$, the rest of the power is sent to the grid (indicated by negative grid power) while the storage devices are charging. This is shown in Figure 7(c). At $t_1$, a drop in solar irradiance reduces PV power, leading to a fluctuation in the DC bus voltage. In response, UC supplies the fluctuating demand while the grid provides the average power, ensuring the DC bus voltage remains stable, as seen in Figure 7(a). Meanwhile, both the battery and UC are charging. At $t_2$, the battery current is nullified, as presented in Figure 7(b) because $SoC_{bt}$ has reached its maximum safe threshold, as shown in Figure 10(a). This action aims to protect the battery from overcharging. The grid addresses average power demand while the UC reacts by absorbing transient power. At $t_3$, the battery remains inactive while the grid and the UC respond to system disturbances to achieve DC bus voltage regulation. UC supplies fluctuating power while charging, and the grid provides the average one (grid power is positive).

At $t_4$, SP to DP transition occurs. The battery starts discharging while the UC stops charging. Using α, the grid and battery provide the average power. At $t_5$, a further reduction in PV power causes another fluctuation in the DC bus voltage. The battery and grid share the responsibility for covering the average power demand, while UC meets the fluctuating power requirement. At $t_6$, $SoC_{bt}$ dips to its minimum safe threshold, as depicted in Figure 8(a). UC absorbs the fluctuating power; the grid provides slow energy while the battery current becomes zero to avoid its deep discharging. At $t_7$, the grid and UC absorb average and transient power, respectively, to stabilize the DC bus voltage. The battery remains inactive as $SoC_{bt}$ has achieved its minimum safe threshold, as depicted in Figure 10(b). This action aims to protect the battery from deep discharging. At $t_8$, DP to SP transition occurs. The storage devices resume charging at their rated charging power. At $t_9$, $SoC_{uc}$ hits its maximum safe threshold, as illustrated in Figure 8(b). UC current becomes zero to prevent overcharging. The battery continues charging, and the grid handles system power requirements. At $t_{10}$, only the grid reacts to the change in PV power because the battery is charging and the UC SoC has reached its maximum threshold, as depicted in Figure 11(b).

## 4.2. Overall performance analysis

In DC microgrids, where diverse sources and loads are integrated, achieving the system power balance is crucial. This involves optimizing power distribution among sources and loads to ensure stable, reliable, and smooth

operation across all conditions. The proposed method effectively maintains power balance across all operating modes by efficiently distributing power among sources and loads, preventing interruptions, and minimizing power losses, as illustrated in Figure 7(c). Moreover, the system's response to transient events is critical for preventing power shortages and voltage fluctuation and protecting the battery from fluctuating currents. The ultracapacitor plays a pivotal role in managing such events, with the DC bus voltage being regulated within milliseconds to ensure minimal voltage deviation and maintain stability. This ensures the system's reliability and stability during transient disturbances. Figure 11(a) illustrates the UC's responses to transient events, showing its swift power absorption (charging) and release (discharging), which is essential for maintaining a constant voltage level.

Additionally, storage devices' safe operation is essential for ensuring better performance and longer lifespan. The proposed power management strategy addresses this by using filtration to shield the battery from high-frequency power variations and employing α and the MPMS to ensure that storage devices remain within predefined operational limits. This approach safeguards the storage devices from overcharging and deep discharge, thus reducing the risk of premature degradation and contributing to a longer lifespan.

Furthermore, the proposed inverter control method successfully achieves grid synchronization, which maximizes efficiency and minimizes losses, as depicted in Figure 9. The power factor on the AC grid is maintained at unity, and the total harmonic distortion in grid currents is less than 5%. Finally, seamless transitions at $t_4$ and $t_8$ ensure a continuous power supply. These features demonstrate the proposed method's effectiveness, versatility, reliability, robustness, and efficiency.
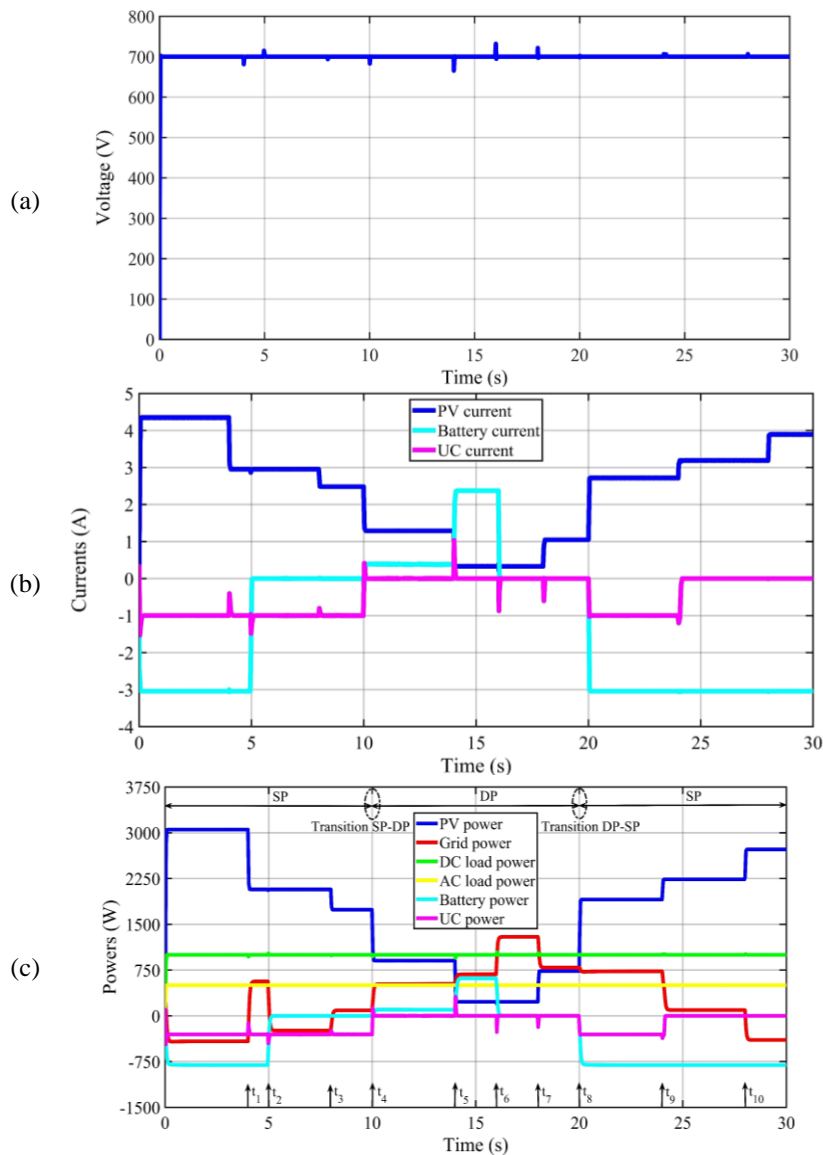


Figure 7. System performance: (a) DC bus voltage, (b) PV, battery, & UC currents, and (c) powers
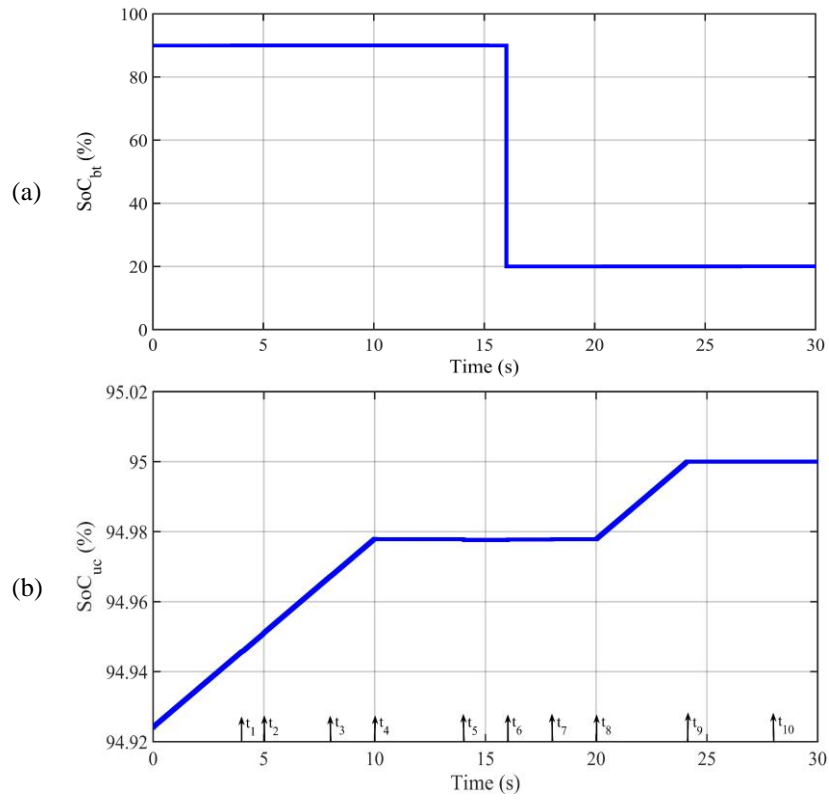
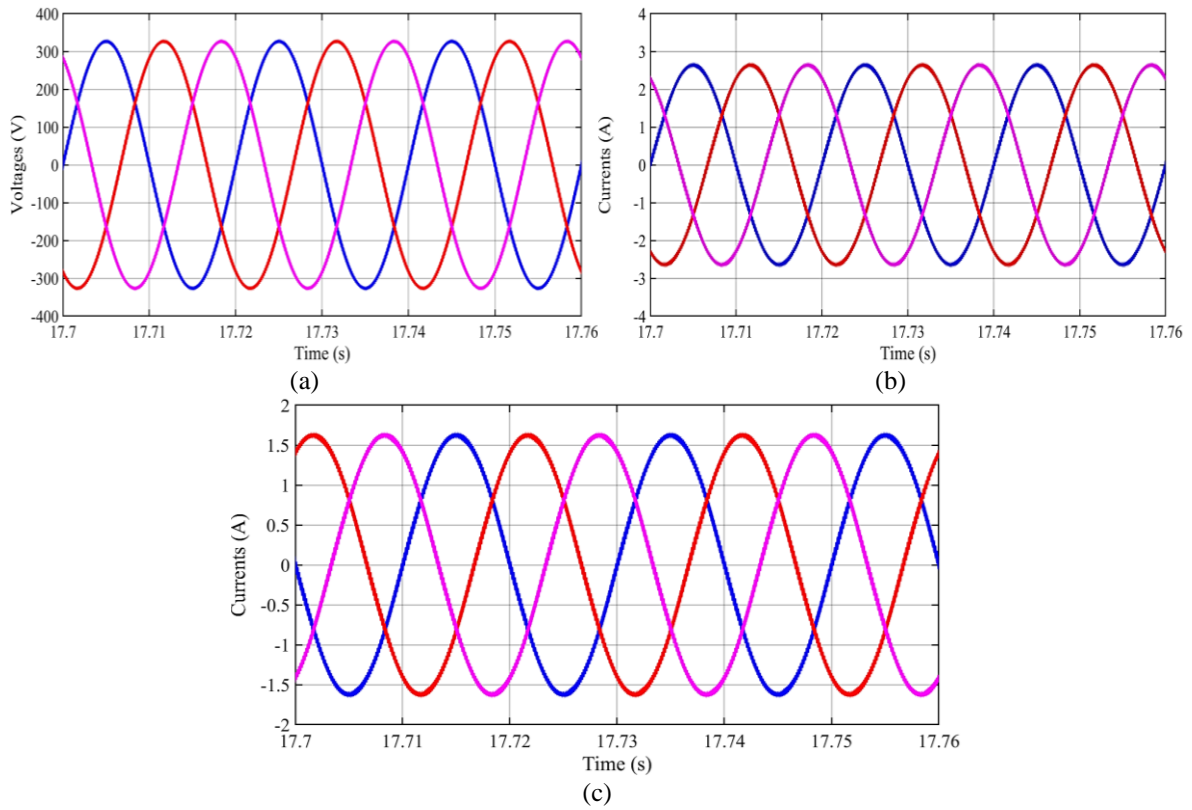Figure 8. System performance: (a) battery SoC and (b) UC SoC



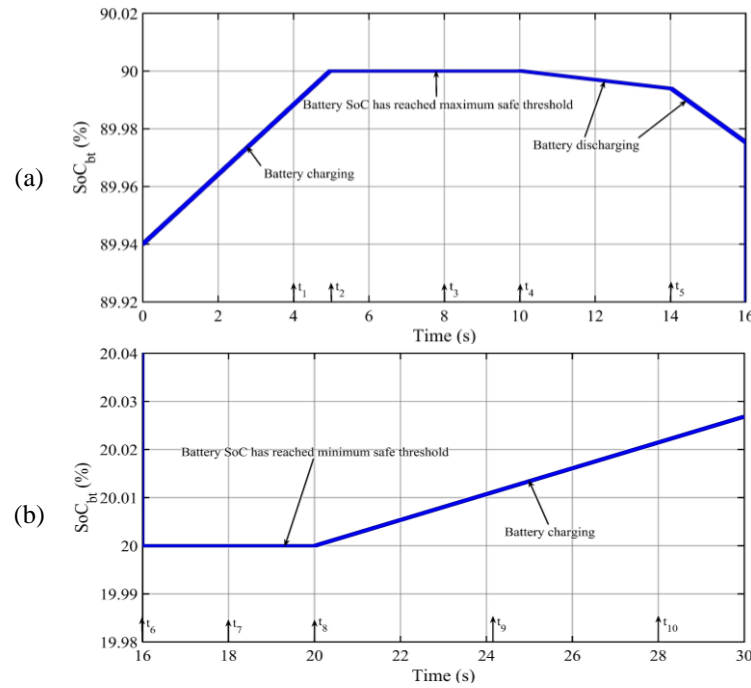Figure 9. System performance: (a) grid voltages, (b) grid currents, and (c) inverter currents

Figure 10. Zoomed view: (a) battery SoC at its maximum safe threshold and (b) battery SoC at its minimum safe threshold
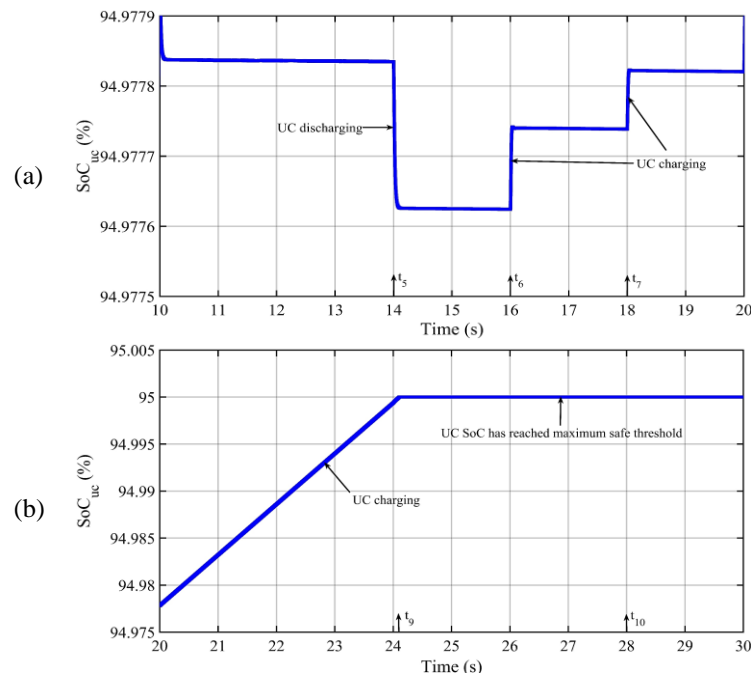


Figure 11. Zoomed view: (a) UC SoC during transient events and (b) UC SoC at its maximum safe threshold

## 5. CONCLUSION

This research introduces an adaptive rule-based power management technique for grid-connected microgrids with battery-ultracapacitor HESS. The strategy integrates the filtration-based method with a microgrid power management system (MPMS) that employs a proportional power allocation factor based on the battery's SoC. The proposed technique is tested under various operating modes with fluctuating generation. Results demonstrate that the method effectively distributes power across all operating modes, ensures smooth transitions between modes, and regulates the DC bus voltage under all conditions. The approach shields the

battery storage from high-frequency power variations and ensures the storage devices operate within safety limits, reducing the risk of premature degradation and potentially extending their lifespan. Additionally, it improves power quality by maintaining the grid power factor to unity. Performance analysis was conducted using MATLAB/Simulink.
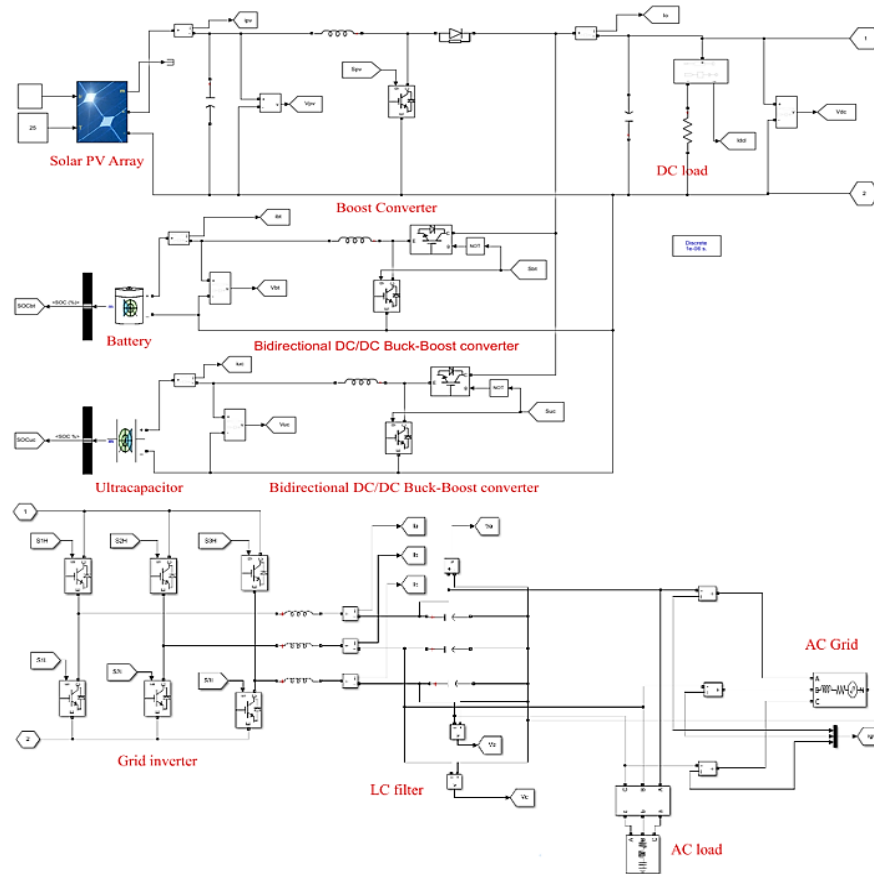
## APPENDIX



Figure 1. Microgrid system simulation setup in MATLAB/Simulink

## REFERENCES

[1]  C. D. Y. de L. Eren Çam, Zoe Hungerford, Niklas Schoch, Francys Pinto Miranda, "Electricity 2024: analysis and forecast to 2026," 2024. [Online]. Available: https://www.iea.org/news/global-coal-demand-expected-to-decline-in-coming-years

[2]  T. Sutikno, W. Arsadiando, A. Wangsupphaphol, A. Yudhana, and M. Facta, "A review of recent advances on hybrid energy storage system for solar photovoltaics power generation," *IEEE Access*, vol. 10, pp. 42346–42364, 2022, doi: 10.1109/ACCESS.2022.3165798.

[3]  S. Barakat, A. Emam, and M. M. Samy, "Investigating grid-connected green power systems' energy storage solutions in the event of frequent blackouts," *Energy Reports*, vol. 8, pp. 5177–5191, 2022, doi: 10.1016/j.egyr.2022.03.201.

[4]  G. G. Farivar *et al.*, "Grid-connected energy storage systems: state-of-the-art and emerging technologies," *Proceedings of the IEEE*, vol. 111, no. 4, pp. 397–420, 2023, doi: 10.1109/JPROC.2022.3183289.

[5]  A. N. Abdalla *et al.*, "Integration of energy storage system and renewable energy sources based on artificial intelligence: an overview," *Journal of Energy Storage*, vol. 40, 2021, doi: 10.1016/j.est.2021.102811.

[6]  A. Fatih Guven, A. Y. Abdelaziz, M. Mahmoud Samy, and S. Barakat, "Optimizing energy dynamics: a comprehensive analysis of hybrid energy storage systems integrating battery banks and supercapacitors," *Energy Conversion and Management*, vol. 312, 2024, doi: 10.1016/j.enconman.2024.118560.

[7]  K. M. Tan, T. S. Babu, V. K. Ramachandaramurthy, P. Kasinathan, S. G. Solanki, and S. K. Raveendran, "Empowering smart grid: a comprehensive review of energy storage technology and application with renewable energy integration," *Journal of Energy Storage*, vol. 39, 2021, doi: 10.1016/j.est.2021.102591.

[8]  J. I. Leon, E. Dominguez, L. Wu, A. Marquez Alcaide, M. Reyes, and J. Liu, "Hybrid energy storage systems: concepts, advantages, and applications," *IEEE Industrial Electronics Magazine*, vol. 15, no. 1, pp. 74–88, 2021, doi: 10.1109/MIE.2020.3016914.

[9]  M. S. Hassan, S. Hassan, M. R. M. Hassan, A. H. M. El-Sayed, M. Shoyama, and G. M. Dousoky, "Performance improvement of a standalone pv system using supercapacitors: modeling and energy management," *International Journal of Power Electronics and Drive Systems*, vol. 15, no. 1, pp. 222–238, 2024, doi: 10.11591/ijpeds.v15.i1.pp222-238.

[10]  M. E. Şahin and F. Blaabjerg, "A hybrid pv-battery/supercapacitor system and a basic active power control proposal in MATLAB/Simulink," *Electronics (Switzerland)*, vol. 9, no. 1, 2020, doi: 10.3390/electronics9010129.

[11] Y. Wang, L. Wang, M. Li, and Z. Chen, "A review of key issues for control and management in battery and ultra-capacitor hybrid energy storage systems," *eTransportation*, vol. 4, 2020, doi: 10.1016/j.etran.2020.100064.

[12] G. A. Ramos and R. Costa-Castelló, "Energy management strategies for hybrid energy storage systems based on filter control: analysis and comparison," *Electronics (Switzerland)*, vol. 11, no. 10, 2022, doi: 10.3390/electronics11101631.

[13] S. Neelagiri and P. Usha, "Modelling and control of grid connected microgrid with hybrid energy storage system," *International Journal of Power Electronics and Drive Systems (IJPEDS)*, vol. 14, no. 3, p. 1791, 2023, doi: 10.11591/ijpeds.v14.i3.pp1791-1801.

[14] M. Z. Zizoui, M. F. Zia, B. Tabbache, Y. Amirat, A. Mamoune, and M. Benbouzid, "Photovoltaic-battery-ultracapacitor-diesel hybrid generation system for mobile hospital energy supply," *Electronics (Switzerland)*, vol. 11, no. 3, 2022, doi: 10.3390/electronics11030390.

[15] P. Singh and J. S. Lather, "Power management and control of a grid-independent dc microgrid with hybrid energy storage system," *Sustainable Energy Technologies and Assessments*, vol. 43, 2021, doi: 10.1016/j.seta.2020.100924.

[16] G. Oriti, N. Anglani, and A. L. Julian, "Hybrid energy storage control in a remote military microgrid with improved supercapacitor utilization and sensitivity analysis," *IEEE Transactions on Industry Applications*, vol. 55, no. 5, pp. 5099–5108, 2019, doi: 10.1109/TIA.2019.2923380.

[17] V. T. Nguyen and J. W. Shim, "Virtual capacity of hybrid energy storage systems using adaptive state of charge range control for smoothing renewable intermittency," *IEEE Access*, vol. 8, pp. 126951–126964, 2020, doi: 10.1109/ACCESS.2020.3008518.

[18] M. F. Elmorshedy, M. R. Elkadeem, K. M. Kotb, I. B. M. Taha, and D. Mazzeo, "Optimal design and energy management of an isolated fully renewable energy system integrating batteries and supercapacitors," *Energy Conversion and Management*, vol. 245, 2021, doi: 10.1016/j.enconman.2021.114584.

[19] A. Aktaş and Y. Kırçiçek, "A novel optimal energy management strategy for offshore wind/marine current/battery/ultracapacitor hybrid renewable energy system," *Energy*, vol. 199, 2020, doi: 10.1016/j.energy.2020.117425.

[20] J. Faria, J. Pombo, M. do Rosário Calado, and S. Mariano, "Power management control strategy based on artificial neural networks for standalone pv applications with a hybrid energy storage system," *Energies*, vol. 12, no. 5, 2019, doi: 10.3390/en12050902.

[21] P. Singh and J. S. Lather, "Accurate power-sharing, voltage regulation, and soc regulation for lvdc microgrid with hybrid energy storage system using artificial neural network," *International Journal of Green Energy*, vol. 17, no. 12, pp. 756–769, 2020, doi: 10.1080/15435075.2020.1798767.

[22] M. Zhang, Q. Xu, C. Zhang, L. Nordström, and F. Blaabjerg, "Decentralized coordination and stabilization of hybrid energy storage systems in dc microgrids," in *2023 IEEE Power & Energy Society General Meeting (PESGM)*, IEEE, Jul. 2023, p. 1. doi: 10.1109/PESGM52003.2023.10253066.

[23] H. Chen, R. Xiong, C. Lin, and W. Shen, "Model predictive control based real-time energy management for hybrid energy storage system," *CSEE Journal of Power and Energy Systems*, vol. 7, no. 4, pp. 862–874, 2021, doi: 10.17775/CSEEJPES.2020.02180.

[24] U. R. Nair and R. Costa-Castello, "A model predictive control-based energy management scheme for hybrid storage system in islanded microgrids," *IEEE Access*, vol. 8, pp. 97809–97822, 2020, doi: 10.1109/ACCESS.2020.2996434.

[25] H. Fallah Ghavidel and S. M. Mousavi-G, "Modeling analysis, control, and type-2 fuzzy energy management strategy of hybrid fuel cell-battery-supercapacitor systems," *Journal of Energy Storage*, vol. 51, 2022, doi: 10.1016/j.est.2022.104456.

[26] R. Zahedi and M. M. Ardehali, "Power management for storage mechanisms including battery, supercapacitor, and hydrogen of autonomous hybrid green power system utilizing multiple optimally-designed fuzzy logic controllers," *Energy*, vol. 204, 2020, doi: 10.1016/j.energy.2020.117935.

[27] S. Sinha and P. Bajpai, "Power management of hybrid energy storage system in a standalone dc microgrid," *Journal of Energy Storage*, vol. 30, 2020, doi: 10.1016/j.est.2020.101523.

[28] S. A. Sarang *et al.*, "Maximizing solar power generation through conventional and digital mppt techniques: a comparative analysis," *Scientific Reports*, vol. 14, no. 1, 2024, doi: 10.1038/s41598-024-59776-z.

[29] D. B. W. Abeywardana, B. Hredzak, V. G. Agelidis, and G. D. Demetriades, "Supercapacitor sizing method for energy-controlled filter-based hybrid energy storage systems," *IEEE Transactions on Power Electronics*, vol. 32, no. 2, pp. 1626–1637, 2017, doi: 10.1109/TPEL.2016.2552198.

[30] E. M. Molla and C. C. Kuo, "Voltage sag enhancement of grid connected hybrid pv-wind power system using battery and smes based dynamic voltage restorer," *IEEE Access*, vol. 8, pp. 130003–130013, 2020, doi: 10.1109/ACCESS.2020.3009420.

# BIOGRAPHIES OF AUTHORS

**Yaya Kamagaté** obtained his bachelor's degree in Electrical and Electronics Engineering from Université Félix Houphouet-Boigny, Abidjan, Côte d'Ivoire, in 2015. He received his master of technology degree in Electrical Engineering from Parul University in 2020. He is currently pursuing a Ph.D. degree in Electrical Engineering at Parul University under the supervision of Dr. Heli Amit Shah. His research interests focus on renewable energy, microgrid control, energy storage, and power quality. He can be contacted at email: 200300418001@paruluniversity.ac.in.

**Heli Amit Shah** received her bachelor of engineering degree in Electrical Engineering in 2003 and received her master of engineering degree in Electrical Engineering in Automatic Control and Robotics in 2005 from the Faculty of Engineering and Technology, Maharaja Sayajirao University of Baroda. She completed her Ph.D. in Power Electronics, Drives, and Embedded Systems from Sardar Vallabhbhai National Institute of Technology, Surat, India, in the year 2015. She served as an associate professor at BITS Edu Campus and is currently a Professor and Head of the Mechatronics/Robotics and Automation Engineering department at Parul Institute of Technology, Parul University. Dr. Shah has 16+ years of academic experience and is guiding several M.Tech./Ph.D. students. Her research areas include power electronics, drives and embedded systems, and renewable energy. She can be contacted at email: heli.shah165006@paruluniversity.ac.in.